JOURNAL OF MATERIALS SCIENCE 11 (1976) 2189–2197

The determination of the extensional compliance perpendicular to the plane of sheet for thin polyethylene terephthalate sheets

I. WILSON*, A. CUNNINGHAM†, R. A. DUCKETT, I. M. WARD
Department of Physics, University of Leeds, Leeds, UK

The extensional compliance normal to the plane of the sheet has been determined for one-way drawn polyethylene terephthalate (PET) sheet. The method was to measure the compressional strain of narrow strips under load in a compressional creep apparatus. It was established that the strips were fully constrained by friction, and a theoretical analysis in support of this is presented. The values for the compliance constant are discussed with regard to the other compliance constants of the PET sheet and are also compared with previous data for PET fibres.

1. Introduction

This paper forms one of a series describing the determination of the nine independent compliance constants for one-way drawn PET sheet. It deals with the measurement of the compliance constant which relates to extension and compression in the direction normal to the plane of the sheet. The principle of the method is to measure the compression of narrow strips under applied load in a compressional creep apparatus. In order to calculate the required compliance constant from the measurements it is necessary to establish the exact mechanics of the compression experiment, i.e. to what extent the samples are constrained by frictional forces. This was examined experimentally by making measurements on strips of different shapes. A theoretical analysis of the problem is also presented.

Finally, the value for this compliance constant is considered in relation to the other compliance constants for this sheet, and the corresponding compliance constants of PET fibre monofilaments.

2. Theory

2.1. The compression experiment

In the compression experiment a narrow strip of the PET sheet is compressed between two steel plates whose dimensions are comparatively very much larger. Any distortion of the plates can be assumed to be negligible as indications from measurements of the transverse compliance of PET monofilaments suggest that the relevant polymer compliance will be about 100 times greater than that of steel. This assumption is confirmed by the results obtained here.

2.2. Theoretical considerations

Rectangular cartesian co-ordinates (1, 2, 3) will be adopted with components of stress σ_1, σ_2, ..., σ_6 and components of strain ϵ_1, ϵ_2, ..., ϵ_6. The compression experiment is shown diagramatically in Fig. 1. The sample shown is a narrow strip which is long in the 3 direction. As discussed previously, the one-way drawn PET sheets possess orthorhombic symmetry. We will consider first the case

*Present address: Toll Bar Comprehensive School, Grimsby, UK.
†Present address: I.C.I. Corporate Laboratory, Runcorn, UK.

© 1976 Chapman and Hall Ltd. Printed in Great Britain.

where the length of the strip is parallel to the initial draw direction; this is the 3 direction. The 1 direction is in the plane of the sheet perpendicular to the draw direction, and the 2 direction is parallel to the axis of compression. The constitutive relations (see, for example [1]) are

$$\epsilon_1 = S_{11}\sigma_1 + S_{12}\sigma_2 + S_{13}\sigma_3$$
$$\epsilon_2 = S_{12}\sigma_1 + S_{22}\sigma_2 + S_{23}\sigma_3$$
$$\epsilon_3 = S_{13}\sigma_1 + S_{13}\sigma_2 + S_{33}\sigma_3 \quad (1)$$

(together with $\epsilon_4 = S_{44}\sigma_4$, $\epsilon_5 = S_{55}\sigma_5$, $\epsilon_6 = S_{66}\sigma_6$, which will not concern us in this paper).

If a long narrow strip is compressed in this manner and if frictional constraints in the 1 direction can be ignored, the situation is one of plane strain, i.e. zero strain in the 3 direction. In this case it may readily be shown that the compressive strain ϵ_2 is related to the applied compressive stress by

$$\epsilon_2 = \left(S_{22} - \frac{S_{23}^2}{S_{33}}\right)\sigma_2 . \quad (2)$$

Similarly, for a narrow strip cut parallel to the one direction the relationship between compressive strain and stress is

$$\epsilon_2 = \left(S_{22} - \frac{S_{12}^2}{S_{11}}\right)\sigma_2 . \quad (3)$$

These results show that if there are no frictional constraints in the narrow direction, experiments comparing the compression response for these two types of strip will reveal differences, provided that S_{23}^2/S_{33} is appreciably different from S_{12}^2/S_{11} and that either or both of these quantities is comparable to S_{22}. For one-way drawn PET sheet the other experiments mentioned in the introduction show that $(S_{12}^2/S_{11}) \sim (10S_{23}^2/S_{33})$.

An alternative assumption is that the width of the strip is sufficiently large compared with its thickness that the frictional constraints provide full constraint, i.e. zero strain in the 1 direction as well as in the 3 direction. For this case it can be shown that the compression is given by

$$\epsilon_2 = \left[S_{22} + \frac{S_{12}(S_{13}S_{23} - S_{12}S_{33}) - S_{23}(S_{11}S_{23} - S_{12}S_{13})}{(S_{11}S_{33} - S_{13}^2)} \right]\sigma_2 \quad (4)$$

For this completely constrained situation we have $\sigma_2 = C_{22}\epsilon_2$, which leads directly to Equation 4. This relationship of course applies for sheets of any shape, i.e. strips cut parallel to either the 1 or 3 direction in these experiments.

It is difficult to appreciate the practical implications of these different assumptions without making a numerical comparison for particular values of the compliance constants. It is, therefore, valuable to substitute the measured room temperature values for the compliance constants S_{11}, S_{33}, S_{12}, S_{13} and S_{23}. These have been obtained from other experiments which have recently been completed [2, 3]. For the assumption of plane strain this gives

$$\epsilon_2 = (S_{22} - 0.18)\sigma_2 \quad (2a)$$

and

$$\epsilon_2 = (S_{22} - 3.6)\sigma_2 \quad (3a)$$

for narrow strips cut parallel to the 3 and 1 directions respectively. If the samples are fully constrained the result is

$$\epsilon_2 = (S_{22} - 4.0)\sigma_2 . \quad (4a)$$

In these equations the units of S_{22} are 10^{-10} $m^2\ N^{-1}$.

Comparison of Equations 2a, 3a and 4a shows that if the samples are not fully constrained we would expect to find a difference between results for strips cut parallel to the 1 and 3 directions, provided that S_{22} is not very much greater than ~ 3 to $4 \times 10^{-10}\ Nm^{-2}$.

2.3. Elastic analysis of plane strain compression with frictional constraints of an anisotropic sheet

Consider the compression of a strip of polymer sufficiently long that one can assume zero elongation parallel to the long axis of the strip Fig. 1). The width of the strip is taken to be $2w$ and thickness h. The analysis will be for a strip

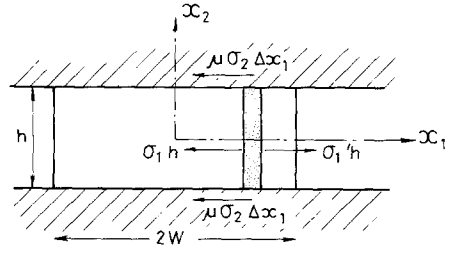

Figure 1 The compression experiment.

cut with its length parallel to the 3 direction; the solution for the other geometry (length parallel to the 1 direction) can be deduced simply by permuting the suffices 1 and 3.

Assume that the sheet is sufficiently thin that variations in stress and strain along the 2 direction can be neglected. Consideration of the equilibrium of unit length of a thin strip of material (shown shaded in Fig. 1) requires that

$$h(\sigma_1' - \sigma_1) = -2\mu\sigma_2 \Delta x_1$$

where μ is the coefficient of friction between the specimen and the steel plates. Since

$$\sigma_1' = \sigma_1(x_1 + \Delta x_1) = \sigma(x_1) + \frac{d\sigma_1}{dx_1} \Delta x_1 + \ldots$$

it follows that

$$\frac{d\sigma_1}{dx_1} = \frac{-2\mu}{h}\sigma_2(x_1). \quad (5)$$

The assumption of plane strain with $\epsilon_3 = 0$ implies from Equation 1 that

$$\sigma_3 = -\frac{(S_{13}\sigma_1 + S_{33}\sigma_2)}{S_{33}}$$

It follows further from Equation 1 in Section 2.2 above that

$$\epsilon_2 = \left(S_{12} - \frac{S_{23}S_{13}}{S_{33}}\right)\sigma_1 + \left(S_{22} - \frac{S_{23}^2}{S_{33}}\right)\sigma_2. \quad (6)$$

The steel plates have a stiffness far exceeding that of the polymer and so we assume that they are undeformed. This is equivalent to the assumption $(d\epsilon_2/dx_1) = 0$ and so from Equation 6 we have

$$\frac{d\sigma_1}{dx_1} = -\frac{(S_{22}S_{33} - S_{23}^2)}{(S_{12}S_{33} - S_{23}S_{13})}\frac{d\sigma_2}{dx_1}. \quad (7)$$

Substitution of Equation 7 into Equation 5 yields

$$\frac{d\sigma_2}{dx_2} = \frac{2\mu}{h}\frac{(S_{11}S_{33} - S_{23}S_{13})}{(S_{22}S_{33} - S_{23}^2)}\sigma_2 \quad (9)$$

and hence

$$\sigma_2(x_1) = Ae^{-\lambda_3 x_1} \quad (10)$$

where

$$\lambda_3 = \frac{(S_{23}S_{13} - S_{12}S_{33})}{(S_{22}S_{33} - S_{23}^2)}\frac{2\mu}{h}. \quad (11)$$

At the edge of the strip ($x_1 = w$), $\sigma_1 = 0$ and so from Equation 6

$$\epsilon_2 = \left(S_{22} - \frac{S_{23}^2}{S_{33}}\right)\sigma_2(w).$$

Hence $A = \epsilon_2 e^{\lambda_3 W}/(S_{22} - S_{33}^2)$ and, therefore, the stress at any point $x_1 > 0$ can be written as

$$\sigma_2(x_1) = \frac{\epsilon_2 e^{-\lambda_3(x_1 - w)}}{(S_{22} - S_{23}^2/S_{33})}. \quad (12)$$

By symmetry the stress for $x_1 < 0$ is

$$\sigma_2(x_1) = \frac{\epsilon_2 e^{\lambda_3(x_1 + w)}}{(S_{22} - S_{23}^2/S_{33})}. \quad (12a)$$

A similar variation in stress in compression specimens at yield has long been recognized and is described as the "friction hill" (see, for example, Cottrell [4].

In this experiment the nominal stress is calculated from the applied load/unit length of strip, P, as

$$\sigma_{\text{nominal}} = P/2w = \frac{1}{2w}\int_{-w}^{w}\sigma_2(x_1)dx_1 \quad (13)$$

On substituting for $\sigma_2(x_1)$ from Equations 12 and 12a and then integrating we obtain an expression for the apparent compliance $\bar{S}_3$ for a strip cut with its long axis parallel to x_3

$$\bar{S}_3 = \epsilon_2/\sigma_{\text{nominal}} = (S_{22} - S_{23}^2/S_{33})\frac{\lambda_3 w}{(e^{\lambda_3 w} - 1)}. \quad (14)$$

It follows from a simple permutation 1↔3 that the apparent compliance $\bar{S}_1$ for a strip cut with its long axis parallel to x_1 is

$$\bar{S}_1 = (S_{22} - S_{12}^2/S_{11})\frac{\lambda_1 w}{(e^{\lambda_1 w} - 1)} \quad (15)$$

where

$$\lambda_1 = \frac{(S_{12}S_{13} - S_{23}S_{11})}{(S_{22}S_{11} - S_{21}^2)} \cdot \frac{2\mu}{h}. \quad (16)$$

Inspection of Equations 11, 14, 15 and 16 reveals several important features. (1) The apparent compliance in both geometries ($\bar{S}_1$ and $\bar{S}_3$) should in general depend on the specimen dimensions through a term of the form $f(\lambda w) = \lambda w/(e^{\lambda w} - 1)$. Note that as $\mu \to 0$, $f(\lambda w) \to 1$ showing that

the apparent compliance should be independent of dimensions in the absence of friction as expected. (2) As the coefficient of friction, μ, increases the apparent compliance appears to decrease without limit. Clearly, for sufficiently high values of μ the specimen will be fully constrained, and the apparent compliance will have a minimum value $\bar{S}_{fc}$ which can be deduced from Equation 4

$$\bar{S}_{fc} = S_{22} + S_{12}(S_{13}S_{23} - S_{12}S_{23}) - \frac{S_{23}(S_{11}S_{23} - S_{12}S_{13})}{(S_{11}S_{33} - S_{13}^2)} \quad (17)$$

(3) It is not possible to obtain an analytical expression for S_{22} from the apparent compliance and a knowledge of the five other compliances S_{21}, S_{23}, S_{13}, S_{11} and S_{33} using either of Equations 14 or 15 since λ_3 and λ_1 both depend on S_{22} itself. This point will be taken up again in the discussion.

3, Experimental

3.1. Preparation of samples

Rectangular samples were cut with their sides parallel to the 1 and 3 directions of the sheet. The sample edges were microtomed and their dimensions determined with a micrometer. The samples, whose dimensions are given in Table I, form two sets according to whether their longest side is parallel to the 1 or the 3 direction.

With a view to eventually extending the measurements to higher temperatures, a set of samples annealed for 6 h at 180° C was also included.

3.2. The compression apparatus

The compression experiment involves the measurement of small deformations ($\sim 10^{-4}$ cm) for the application of comparatively large loads to the sample (~ 20 kg). It was therefore necessary to use a specially constructed dead-loading creep apparatus based on a design developed by Imperial Chemical Industries, Plastic Division, Welwyn Garden City [5]. This is shown schematically in Fig. 2.

The load is applied to the compression cage A, via two lever arms pivoted about a common fulcrum B. The load is placed on the weight pan at the end of the larger lever arm C, and supported by the rod D. This rod is held in position by an electromagnet, and until released, prevents the load from being applied to the sample.

The short lever arm is then adjusted until it makes contact with the long lever arm at the point E. Loads added to the short lever arm are used to balance the compression cage, and can also apply a pre-load. When the system has been carefully balanced and loaded, the required load is applied to the compression cage by switching off the electromagnet.

Because the apparatus was designed for the compression of much thicker samples, an intermediate steel spacer 3 cm long and 2 cm diameter was inserted in the compression cage as shown (P). To improve the accuracy of the measure-

TABLE I Collected data from compression experiments.

Sample shape	Sample state and number		Width (cm)	Length (cm)	Apparent compliance ($\times 10^{-10}$ m^2 N^{-1})	Average apparent compliance ($\times 10^{-10}$ m^2 N^{-1})
Length of strip parallel to draw direction	Unannealed	(1)	0.30	1.64	4.7	
		(2)	0.40	1.60	5.3	4.8 ± 0.4
		(3)	0.09	1.54	4.8	
		(4)	0.15	1.55	4.3	
	Annealed	(5)	0.09	1.57	4.6	
		(6)	0.25	1.20	3.4	3.9 ± 0.5
		(7)	0.40	1.11	3.7	
Length of strip perpendicular to draw direction	Unannealed	(8)	0.31	1.69	5.3	
		(9)	0.42	1.26	5.6	5.15 ± 0.5
		(10)	0.11	1.68	5.4	
		(11)	0.20	1.47	4.3	
	Annealed	(12)	0.08	1.16	3.5	
		(13)	0.32	1.21	3.5	3.7 ± 0.3
		(14)	0.42	1.21	4.2	

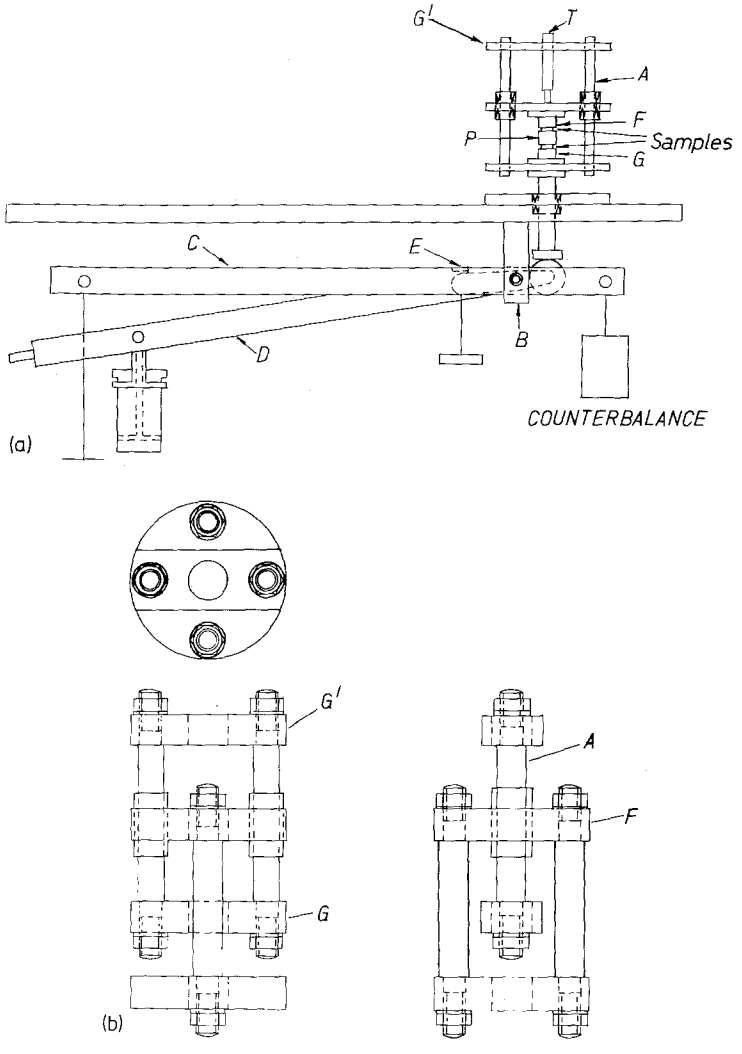

Figure 2 The compression apparatus: (a) overhead projection, (b) end elevation.

ments, two identical samples were compressed in each experiment; between the top of the spacer and the upper face of the compression cage and between the bottom of the spacer and the lower face of the compression cage respectively.

The top compression face F is fixed, and when the load is applied, the bottom face G moves upwards carrying the framework G′. The displacement was measured by the transducer T which is attached to G′ and contacts on the upper surface of the compression face F.

3.3. Calibration and measurements

In the first instance the transducer was calibrated for displacements up to 2×10^{-3} cm using a micrometer screw gauge. The apparatus compliance was then determined from measurements of the deformation of the compression cage under load, with only the steel spacer between the compression faces. The results, shown in Fig. 3, indicate that there is a linear relationship between the compression cage deformation and applied load. In the subsequent compression experiments on the sheet, this machine deformation was therefore subtracted from the measured deformation to give the sample deformation. The machine deformation was about one-third of the total deformation, and this factor clearly limits the accuracy of the experiments.

The apparatus was initially set up with the sheet samples in position, and the load on the short lever arm such as to balance the weight of the compression cage. Typical plots of the relative contraction (sample contraction divided by sample

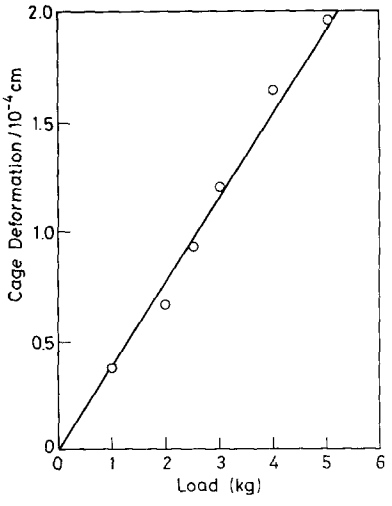

Figure 3 Calibration of machine compliance: cage deformation versus applied load.

thickness, after correction for machine compliance) as a function of applied load are shown in Fig. 4. The plots show appreciable curvature which is due to a combination of slight unevenness in sample thickness and minor misalignment of the compression cage. The effects of this curvature can be eliminated by the adoption of a pre-load of at least 2 kg.

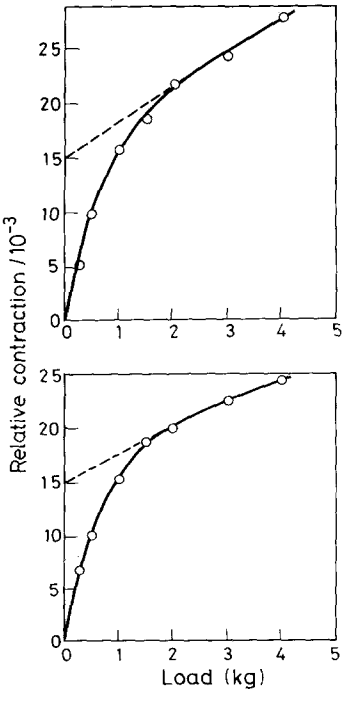

Figure 4 Relative contraction as a function of applied load for a small dead load.

4. Results and discussion

Measurements were made on unannealed and annealed sheets of different dimensions. Typical results are shown in Figs. 5 to 8 and the data are summarized in Table I. In all cases a good linear relationship was observed between the contraction of the sheet and the applied load. The apparent compliance (sample strain divided by nominal stress) was calculated for each experiment and the results are shown in Table I. It is clear that for each group of tests there is no significant dependence on sample dimension. For example the coefficients of correlation between apparent compliance and specimen width for the unannealed materials are −0.22 and −0.02 for specimens cut in the 3 and 1 directions respectively.

Furthermore there is no significant difference between the two specimen orientations for either unannealed or annealed materials. A simple statistical analysis shows that there is greater than 70% probability that both sets of data on the unannealed material are from the same population, but of course the restricted amount of data from this and especially from the annealed material make a more complete analysis difficult to justify. There would appear to be a systematic difference between the two materials, but since the other compliance constants are not yet available for the annealed material further analysis of those data is not possible.

Returning to the unannealed material we must assume that the specimens in both directions are always fully constrained by friction. This is the only way of rationalizing the two observations that (1) there is no dependence of compliance on dimensions in either orientation and (2) the compliance is identical in the two orientations.

Thus we take $\bar{S}_{fc} = (5.0 \pm 0.5) \times 10^{-10}$ m^2 N^{-1} and calculate a value of S_{22} to be $(9.0 \pm 1.7) \times 10^{-10}$ m^2 N^{-1} using Equation 17 and values of S_{12}, S_{23}, S_{13}, S_{11} and S_{33} determined independently (see Table II). The larger error in the final value of S_{22} arises from the additional errors in the other compliance constants. Comparison of this

TABLE II Collected values of compliance constants ($\times 10^{-10}$ m^2 N^{-1})

	S_{11}	S_{22}	S_{33}	S_{21}	S_{23}	S_{13}
Unannealed sheet	4.0	9.0	0.76	−3.8	−0.37	−0.18
Fibre elastic Constants A	8.9	8.9	1.1	−3.9	–	−0.47
Fibre elastic Constants B	16.1	16.1	0.71	−5.8	–	−0.31

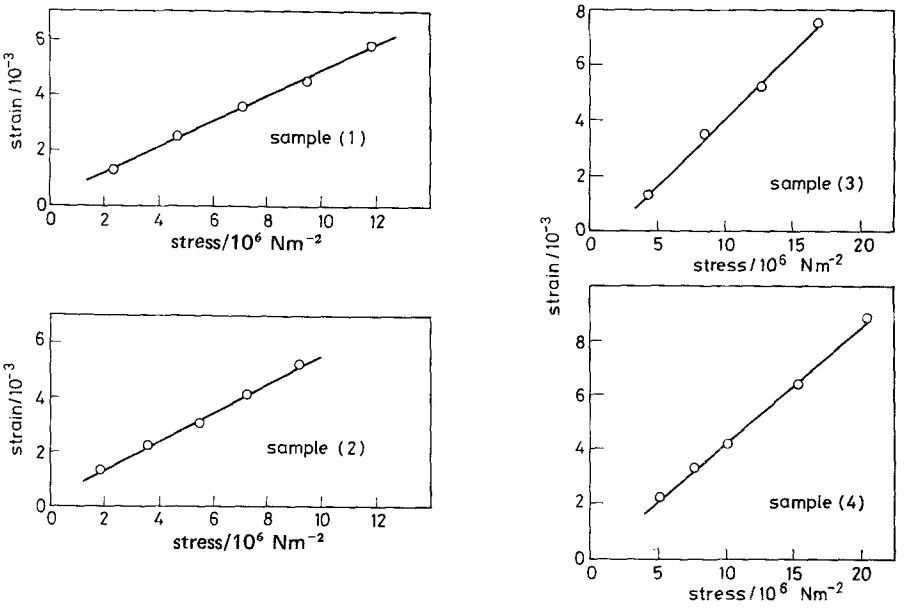

Figure 5 Compressive strain versus applied stress for unannealed strip, length parallel to draw direction. Samples 1 to 4.

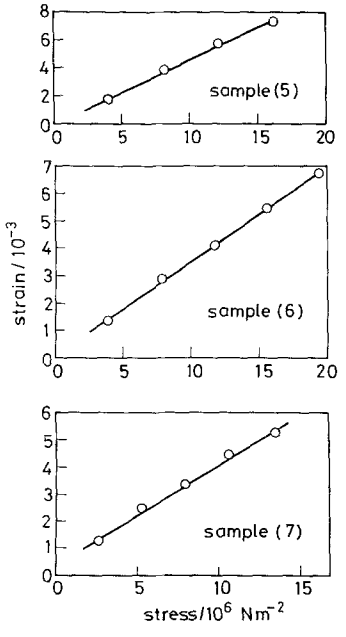

Figure 6 Compressive strain versus applied stress for annealed strip length parallel to draw direction. Samples 5 to 7.

value of S_{22} with S_{11} and transverse compliances previously measured for PET fibres of comparable orientation and crystallinity (also shown in Table II) confirm it to be quite reasonable. It is, however, necessary to test whether the assumption of complete constraint is compatible with the likely values of the coefficient of friction between PET and steel $0.2 < \mu < 0.4$ [6]. In order to test this assumption we have therefore taken Equations 14 and 15 and calculated the expected dependence of the apparent compliances $\bar{S}_1$ and $\bar{S}_3$ for $\mu = 0.2$ and 0.4 using the compliance data in Table II. The results of these calculations are shown in Figs. 9 and 10 from which it can be seen that it is quite reasonable to assume that even the narrowest of specimens in Table I is effectively "fully constrained" by friction.

This result for S_{22} enables us to complete the determination of the compliance constants for unannealed PET sheet and the collected results are shown in Table II. (The shear compliances have been reported in a previous publication [7]. It can be seen that S_{22} has a very similar value to S_{11}, both being much greater than S_{33}. This is an expected result, because S_{33} is likely to involve distortion of bonds in the molecular chains to some extent, whereas S_{11} and S_{22} will relate to dispersion forces between chains. The values of the Poisson's ratio compliances are also entirely consistent with this. S_{21} is of the same order of magnitude as S_{11} and S_{22}, whereas S_{23} and S_{13} are much smaller, again reflecting the lower stiffness of the material in the draw direction.

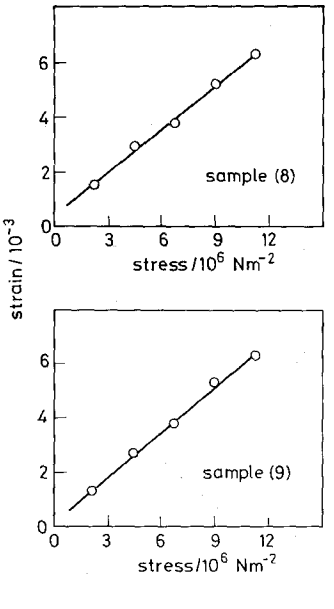

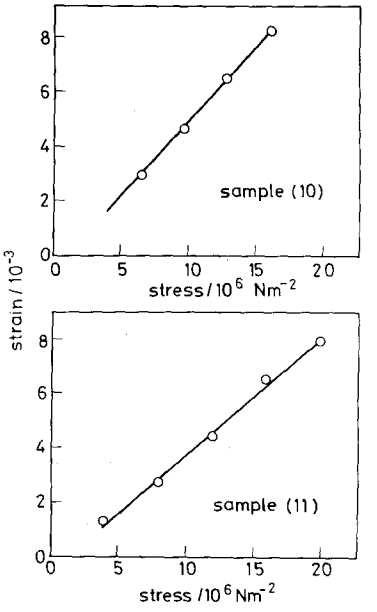

Figure 7 Compressive strain versus applied stress for unannealed strip, length perpendicular to draw direction. Samples 8 to 11.

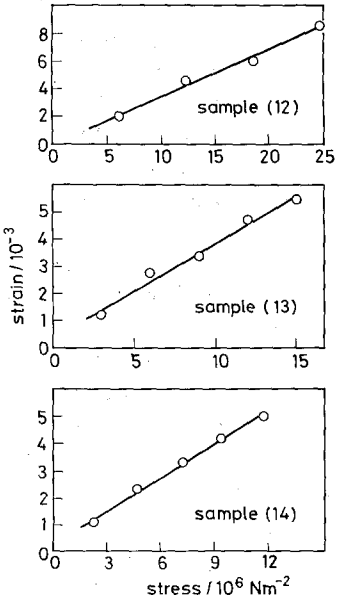

Figure 8 Compressive strain versus applied stress for annealed strip, length perpendicular to draw direction. Samples 12 to 14.

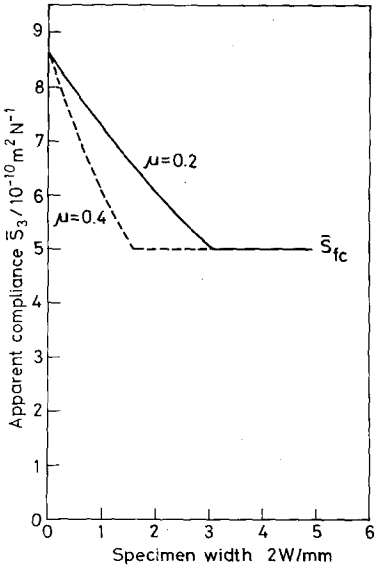

Figure 9 The expected dependence of apparent compliance $\bar{S}_3$ on width for a specimen cut with its long dimension parallel to axis 3. (Calculated from Equation 14 using data from Table II.)

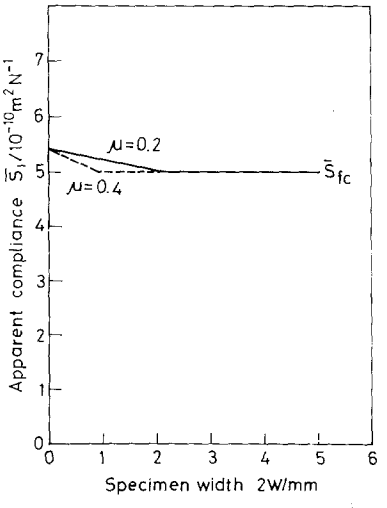

Figure 10 The expected dependence of apparent compliance $\bar{S}_1$ on width for a specimen cut with its long dimension parallel to axis 1. (Calculated from Equation 15 using data from Table II.)

We have already remarked on the comparison between data for sheet and fibres. In this context all the sheet compliances appear reasonable, and do not suggest that there are major structural differences between fibres and sheets, apart from the lower symmetry of the latter. In a review article on the mechanical properties of oriented polymers [8], preliminary results for the compliance constants were quoted, and it was shown that differences of this kind between fibres and sheets can be attributed to differences in overall molecular orientation. The aggregate model, which considers the polymer as an aggregate of anisotropic units, was shown to produce reasonable correlations between the compliance constants of fibres, sheet and unoriented polymer.

Acknowledgement

We are indebted to Dr S. Turner and Miss D.A. Thomas for their advice and assistance on the construction of the dead-loading creep apparatus.

References

1. I. M. WARD, "Mechanical Properties of Solid Polymers" (Wiley, London, 1971) p. 229.
2. I. WILSON, A. CUNNINGHAM and I. M. WARD, *J. Mater. Sci.* **11** (1976) 2188.
3. I. WILSON, N. H. LADIZESKY and I. M. WARD, *ibid* **11** (1976) 2177.
4. A. H. COTTRELL, "The Mechanical Properties of Matter" (Wiley, London, 1964) p. 335.
5. D. A. THOMAS, *Plastics and Polymers* **37** (1969) 485.
6. W. J. ROFF and J. R. SCOTT, "Fibres, films, plastics and rubbers", (Butterworths, London, 1971) p. 245.
7. N. H. LADIZESKY and I. M. WARD, *J. Mater. Sci.* 8 (1973) 980.
8. I. M. WARD, *Polymer* **15** (1974) 379.

Received 13 April and accepted 4 May 1976.